JOURNAL OF COMPUTATIONAL PHYSICS 96, 369–390 (1991)

The Effect of Filtering on the Pseudospectral Solution of Evolutionary Partial Differential Equations

L. S. MULHOLLAND AND D. M. SLOAN

Department of Mathematics, University of Strathclyde, Glasgow G1 1XH, Scotland

Received March 13, 1989; revised May 22, 1990

This paper examines the effect of filtering on the solution of time-dependent partial differential equations by the pseudospectral method. It is shown that if spatial discretisation is effected using the Fourier pseudospectral method the computed solution will be an approximation to the solution of a modified differential equation. The changes in dispersive and dissipative properties induced by the modification are examined, and numerical results are presented which illustrate these changes for both linear and nonlinear equations. Numerical results are also presented which show the effect of filtering on Chebyshev pseudospectral solutions of time-dependent equations. © 1991 Academic Press, Inc.

1. INTRODUCTION

Several authors have used filtering to improve the stability properties of pseudospectral solutions of evolutionary partial differential equations. Here we use the word pseudospectral, as introduced by Orszag [10], to describe a method which differs from a Galerkin method in its treatment of nonlinear terms; in the former, a fully-aliased transform technique is used to evaluate convolution sums. As shown in the text by Canuto *et al.* [2], a pseudospectral method is algebraically equivalent to a collocation method. In this note we use the words pseudospectral and collocation synonymously.

Fornberg and Whitham [4] performed extensive calculations on the Korteweg–de Vries (KdV) equation using a method which combined Fourier collocation in space and a leap-frog discretisation in time. They introduced a form of filter which enabled them to increase the linear stability limit on the time-step by a factor of five. He-Ping Ma and Ben-Yu Guo [7] proposed a Fourier pseudospectral scheme for the KdV equation which contained a filtering device designed to control nonlinear instabilities, and Guo and Cao [1] extended the idea to deal with the regularised long wave equation. Majda, McDonough, and Osher [8] have examined the effect of filtering on the accuracy of Fourier spectral solutions of linear hyperbolic equations. These authors directed their attention to high frequency oscillations induced by a discontinuity in the initial data. They demonstrated that a well-chosen smoothing operator could stabilise an unstable method and that this smoothing, together with a certain smoothing of the initial data, could yield infinite order accuracy away from the discontinuity.

0021-9991/91 $3.00

In the case of collocation approximations of non-periodic solutions the need for filtering appears to be more pronounced. Outlying eigenvalues of first-order Chebyshev pseudospectral differentiation matrices have magnitude $O(N^2)$, where N is the number of collocation points [3]. This leads to time-step stability restrictions of the form $\Delta t = O(N^{-2})$ when integrating first-order hyperbolic systems by an explicit pseudospectral method, and this is much more severe than the $O(N^{-1})$ restriction which applies with finite difference methods. Gottlieb and Turkel [6] proposed a filter which, they claimed, yielded unconditionally stable explicit methods. However, Fulton and Taylor [5] subsequently established that the Gottlieb–Turkel filter could lead to absolute instability for any time-step. Fulton and Taylor suggested that the effect of filtering "is similar to the computational dispersion seen in centred finite difference approximations." This dispersive effect was also noted by Nouri [9] in filtered, pseudospectral solutions of a linear KdV equation.

Weideman and Trefethen [11] examined the effect of filtering on the spectral radius of second-order Chebyshev pseudospectral differentiation matrices. The matrices in this case have outlying eigenvalues of magnitude $O(N^4)$ for large N. Weideman and Trefethen concluded that every filter which they examined led to a loss of accuracy in the low eigenvalues. The aim here is to add a little to the understanding of the physical nature of accuracy loss in pseudospectral solutions of time-dependent partial differential equations which might result from filtering. We are particularly interested in loss of accuracy in smooth solutions brought about by the dispersion and dissipation which is introduced by filtering. In Section 2 we consider Fourier pseudospectral solutions of homogeneous, linear, constant coefficient equations. There it is shown that a filtered solution is a solution of a modified differential equation, and numerical results illustrate the effect of this modification. Numerical results presented in Section 3 show that filtering introduces related changes to non-periodic problems solved by Chebyshev pseudospectral methods. In Section 4 the interplay between nonlinearity and filtering is considered, and conclusions are contained in Section 5.

2. Periodic Solutions of Linear Equations

2.1. *Modifications Induced by Filtering*

Initially we consider the homogeneous, linear, constant coefficient partial differential equation

$$u_t + Lu = 0, \tag{2.1}$$

where $L \equiv \sum_{r=1}^{R} \mu_r D^r$, with $D \equiv \partial/\partial x$ and $\mu_r = \text{const}$ for $r = 1, 2, ..., R$. Suppose that $u(x, t)$ satisfies 2π-periodic initial conditions and the periodic boundary condition

$$u(x + 2\pi, t) = u(x, t), \qquad (x, t) \in \mathbb{R} \times [0, T]. \tag{2.2}$$

To solve this problem by a pseudospectral method the interval $[0, 2\pi]$ is discretised by $N+1$ equidistant points with spacing $\Delta x = 2\pi/N$, and $u(\cdot, t)$ is approximated by $U(\cdot, t) \in \mathbb{R}^N$, which has the value $U(x_j, t)$ at $x = x_j = j\,\Delta x$, $j = 0, 1, ..., N-1$. If N is assumed to be even, with $M = N/2$, the vector $U(\cdot, t)$ is transformed to discrete Fourier space by

$$\hat{U}(p, t) = (FU(\cdot, t))(p) = \frac{1}{\sqrt{N}} \sum_{j=0}^{N-1} U(x_j, t) e^{-2\pi i j p/N}, \qquad p = -M, -M+1, ..., M-1. \tag{2.3}$$

The inversion formula for the discrete transform (2.3) is

$$U(x_j, t) = (F^{-1}\hat{U}(\cdot, t))(x_j) = \frac{1}{\sqrt{N}} \sum_{p=-M}^{M-1} \hat{U}(p, t) e^{2\pi i j p/N}, \qquad j = 0, 1, ..., N-1. \tag{2.4}$$

Transformations (2.3) and (2.4) can be performed efficiently by means of the fast Fourier transform algorithm (FFT). Derivatives of u with respect to x may also be approximated efficiently by the FFT algorithm: for example, the rth derivative at (x_j, t) is given by $(F^{-1}\hat{V}(\cdot, t))(x_j)$, where $\hat{V}(p, t) = (ip)^r \hat{U}(p, t)$. If this is denoted by $U^{(r)}(x_j, t)$, and z denotes the Nth root of unity, $\exp(2\pi i/N)$, then

$$U^{(r)}(x_j, t) = \frac{1}{\sqrt{N}} \sum_{p=-M}^{M-1} (ip)^r \hat{U}(p, t)\, z^{jp}. \tag{2.5}$$

A filtered approximation to the rth derivative is given by

$$U_F^{(r)}(x_j, t) = \frac{1}{\sqrt{N}} \sum_{p=-M}^{M-1} \sigma_p (ip)^r \hat{U}(p, t)\, z^{jp}, \tag{2.6}$$

where σ_p is a real, non-negative filter function satisfying $\sigma_0 = 1$, $\sigma_p = \sigma_{-p}$, and $\sigma_{|p|}$ is a decreasing function of $|p|$. Many of the popular filters may be written in the form

$$\sigma_p = \sum_{s=0}^{\infty} a_s (ip)^{2s}, \qquad a_0 = 1, \tag{2.7}$$

where a_s depends on M: we assume this form in the subsequent analysis. If σ_p in (2.6) is expanded as in (2.7) we obtain

$$\begin{aligned} U_F^{(r)}(x_j, t) &= \frac{1}{\sqrt{N}} \sum_{p=-M}^{M-1} \left[\sum_{s=0}^{\infty} a_s (ip)^{2s} \right] (ip)^r \hat{U}(p, t)\, z^{jp} \\ &= \sum_{s=0}^{\infty} a_s \left[\frac{1}{\sqrt{N}} \sum_{p=-M}^{M-1} (ip)^{r+2s} \hat{U}(p, t)\, z^{jp} \right] \\ &= \sum_{s=0}^{\infty} a_s U^{(r+2s)}(x_j, t), \end{aligned}$$

and this may be written as

$$U_F^{(r)}(x_j, t) = U^{(r)}(x_j, t) + \sum_{s=1}^{\infty} a_s U^{(r+2s)}(x_j, t). \tag{2.8}$$

Note that if $a_s = 0$ for $s > 0$ then $\sigma_p \equiv 1$ and (2.8) reduces to $U_F^{(r)}(x_j, t) = U^{(r)}(x_j, t)$.

If the discretisation of the spatial derivatives in (2.1) is effected using a Fourier pseudospectral method incorporating the filter (2.7), it follows from (2.8) that the semi-discrete equations are effectively

$$\dot{U}(x_j, t) + \sum_{r=1}^{R} \mu_r \left[U^{(r)}(x_j, t) + \sum_{s=1}^{\infty} a_s U^{(r+2s)}(x_j, t) \right] = 0, \tag{2.9}$$

for $j = 0, 1, ..., N-1$, where the dot denotes differentiation with respect to time. (2.9) may be written as

$$\dot{U}(x_j, t) + (LU)(x_j, t) + (L_\sigma U)(x_j, t) = 0, \tag{2.10}$$

where L_σ is the differential operator defined by

$$L_\sigma = \sum_{r=1}^{R} \mu_r \sum_{s=1}^{\infty} a_s D^{r+2s}, \tag{2.11}$$

with $D \equiv \partial/\partial x$. Equation (2.10) shows that, as a result of the filtering, the computed solution may be regarded as an approximation to the 2π-periodic solution of

$$u_t + Lu + L_\sigma u = 0, \tag{2.12}$$

with initial conditions similar to those prescribed for (2.1). The filter has therefore introduced an additional, well-defined spatial operator to the differential equation.

The filter which we use in the computations described later is the exponential filter

$$\sigma_p = e^{-Kp^2} \tag{2.13}$$

in which K is a non-negative constant. This filter may, of course, be expanded as in (2.7) with $a_s = K^s/s!$. Other filters which have been used elsewhere in pseudospectral calculations are the Lanczos filter,

$$\sigma_p = \frac{\sin(2\pi p/N)}{(2\pi p/N)}, \tag{2.14}$$

and the raised cosine filter,

$$\sigma_p = \tfrac{1}{2}[1 + \cos(2\pi p/N)]. \tag{2.15}$$

The filters (2.14) and (2.15) may also be expanded as in (2.7).

Special cases. Particular forms of the constant coefficient, linear equation (2.1) used in numerical illustrations in this section are

(i) the advection equation

$$u_t + \mu u_x = 0, \tag{2.16}$$

(ii) the KdV equation

$$u_t + \mu u_x + \varepsilon u_{xxx} = 0, \tag{2.17}$$

and

(iii) Burgers' equation

$$u_t + \mu u_x - \varepsilon u_{xx} = 0. \tag{2.18}$$

If the pseudospectral derivatives are filtered by means of (2.7) the modified equations associated with (2.16), (2.17), and (2.18) are, respectively,

$$u_t + \mu u_x + \mu \sum_{s=1}^{\infty} a_s u^{(1+2s)} = 0, \tag{2.19}$$

$$u_t + \mu u_x + \varepsilon u_{xxx} + \sum_{s=1}^{\infty} a_s [\mu u^{(1+2s)} + \varepsilon u^{(3+2s)}] = 0 \tag{2.20}$$

and

$$u_t + \mu u_x - \varepsilon u_{xx} + \sum_{s=1}^{\infty} a_s [\mu u^{(1+2s)} - \varepsilon u^{(2+2s)}] = 0. \tag{2.21}$$

Here $u^{(r)}$ denotes the rth spatial derivative of u.

2.2. *Dispersion and Dissipation*

A monochromatic, 2π-periodic solution of (2.1) has the form

$$u(x, t) = Ae^{ip(x - c_p t)}, \tag{2.22}$$

where p is an integer (non-negative), and it is readily shown by substitution in (2.1) that

$$c_p = \sum_{r=1}^{R} \mu_r (ip)^{r-1}. \tag{2.23}$$

The solution of the modified equation (2.12), coincident with (2.22) at $t = 0$, is

$$u_F(x, t) = Ae^{ip(x - d_p t)}, \tag{2.24}$$

and it is readily shown that

$$d_p = c_p \sigma_p. \tag{2.25}$$

This equation gives information on the dispersion and dissipation introduced by the filtering process.

The filtering effect is more readily seen in terms of the three special cases described by (2.16), (2.17) and (2.18). The values of c_p for these models are, respectively,

$$c_p = \mu, \tag{2.26a}$$

$$c_p = \mu - \varepsilon p^2, \tag{2.26b}$$

$$c_p = \mu - i\varepsilon p. \tag{2.26c}$$

If we consider the exponential filter (2.13) the corresponding values of d_p are, respectively,

$$d_p = \mu e^{-Kp^2}, \tag{2.27a}$$

$$d_p = (\mu - \varepsilon p^2) e^{-Kp^2}, \tag{2.27b}$$

$$d_p = (\mu - i\varepsilon p) e^{-Kp^2}. \tag{2.27c}$$

The dispersion-free advection equation has dispersion introduced by the filtering process: the magnitude of the phase velocity is reduced in a frequency-dependent manner and the phase lag is more pronounced at high frequencies. Analogous frequency-dependent phase changes occur in solutions of the KdV equation and the Burgers' equation. The complex terms in c_p and d_p reflect the dissipation in Burgers' equation. In this case the monochromatic solution

$$u(x, t) = Ae^{ip(x-\mu t)} e^{-\varepsilon p^2 t} \tag{2.28}$$

of (2.18) is modified by exponential filtering to

$$u_F(x, t) = Ae^{ip(x-\mu e^{-Kp^2} t)} e^{-\varepsilon p^2 e^{-Kp^2} t}. \tag{2.29}$$

This shows that the damping has actually been diminished by the filtering process. Filtered pseudospectral solutions of a dissipative equation suffer dispersion and a relaxation of the damping.

It should be noted that the group velocity is also modified by pseudospectral filtering. The group velocities associated with (2.22) and (2.24) are defined by $(d/dp)(pc_p)$ and $(d/dp)(pd_p)$, respectively. In the case of the advection equation and the exponential filter, for example, these are given by

$$g_p = \mu \quad \text{and} \quad g_p = \mu(1 - 2Kp^2) e^{-Kp^2}, \tag{2.30a), (2.30b}$$

respectively.

2.3. *Numerical Illustrations*

To illustrate the induced dispersion we considered the pseudospectral solution of the linear KdV equation (2.17). The solution is particularly simple for the monochromatic initial condition

$$U(x_j, 0) = \cos(mx_j), \qquad j = 0, 1, ..., N-1, \tag{2.31}$$

with m an integer in the range $0 < m < M$ $(= N/2)$. The solution of the filtered equation at $t = T$ is

$$U(x_j, T) = \cos[m(x_j - c_m \sigma_m T)], \tag{2.32}$$

with c_m given by (2.26b). The operator modification viewpoint has provided a precise description of the filtering effect in this linear, monochromatic case.

Figures 1a, b show the filtered and unfiltered solutions of the linear KdV equation from initial condition (2.31), with $m = 2$ and $m = 3$ in (a) and (b), respectively. The filtered and unfiltered solutions at time $T = 1$ are represented by the unbroken and broken curves, respectively. Filtering is achieved using the exponential filter (2.13) with $K = \frac{1}{10}$ and the parameters in equation (2.17) are chosen as $\mu = 6$, $\varepsilon = 5/m^2$, so that $c_m = 1$ for each solution. The phase lag of the filtered solution, $1 - \sigma_m$, is seen clearly in the figures.

To illustrate the change in dissipative properties brought about by filtering we considered the filtered pseudospectral solution of the linear Burgers equation (2.18) from the initial condition (2.31). In this case the exact solution of the pseudospectral equations at time $t = T$ is

$$U(x_j, T) = e^{-\sigma_m \varepsilon m^2 T} \cos[m(x_j - \sigma_m \mu T)]. \tag{2.33}$$

The unbroken and broken curves in Figs. 2 show the filtered and unfiltered solutions of (2.18) at $T = 1$. As in the KdV solution we use the exponential filter with $K = \frac{1}{10}$. Figures 2a and b show solutions for $m = 1$ and $m = 2$, respectively, with parameter values $\mu = \varepsilon = 1$ in each case. The phase lag, $1 - \sigma_m$, induced by the filtering is again evident. Furthermore, the diminution of the dissipation is clearly seen. The amplitude of the mode m solution at $t = T$ is increased from $e^{-\varepsilon m^2 T}$ to $e^{-\sigma_m \varepsilon m^2 T}$ by the filtering process. For the parameter set chosen here the change in dissipation is very significant for modes with $m > 2$. For example, at $m = 3$ the amplitude at $T = 1$ is increased from 0.00012 to 0.026 by the filtering process.

Filters (2.14) and (2.15) are very weak for small values of p. However, if these filters are used in pseudospectral calculations it is readily shown that short wavelength modes suffer significant dispersive and dissipative changes like those catalogued above.

Figures 3 are included to illustrate the change in group velocity due to filtering. We considered unfiltered and filtered solutions of the advection equation (2.16), with initial conditions defined by the wave packet

$$U(x_j, 0) = e^{-16(x_j - 1)^2} \sin(mx_j), \qquad j = 0, 1, ..., N-1. \tag{2.34}$$

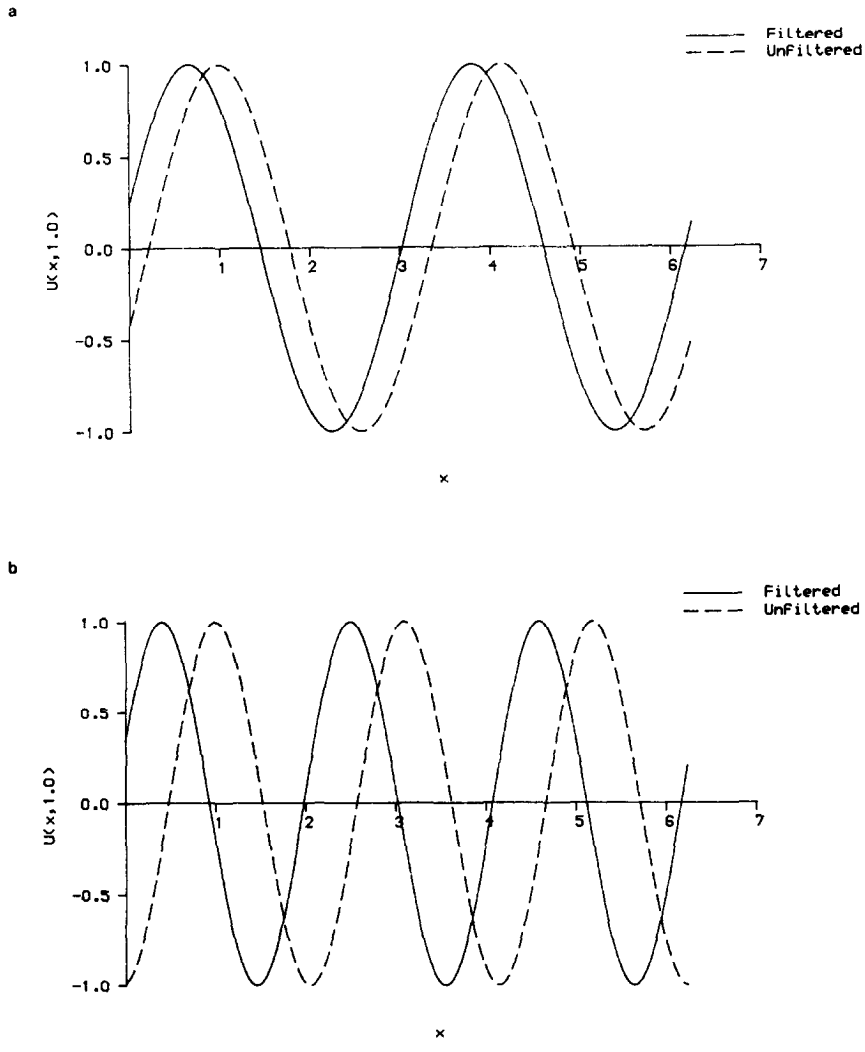

FIG. 1. Filtered and unfiltered solutions of (2.17) at time $T=1$, with initial condition (2.31), $\mu=6$, $\varepsilon=5/\mathrm{m}^2$ and filter (2.13) with $K=0.1$; $m=2$ and $m=3$ in (a) and (b), respectively.

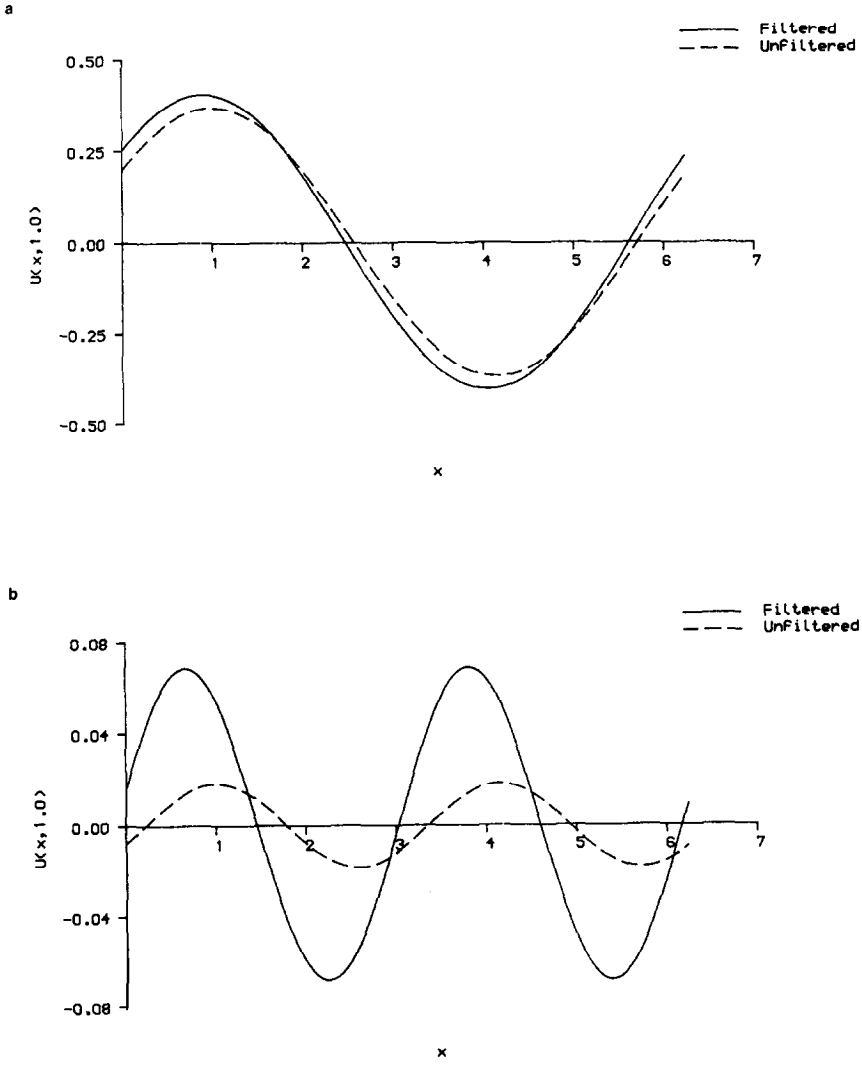

FIG. 2. Filtered and unfiltered solutions of (2.18) at time $T=1$, with initial condition (2.31), $\mu=1$, $\nu=1$ and filter (2.13) with $K=0.1$; $m=1$ and $m=2$ in (a) and (b), respectively.

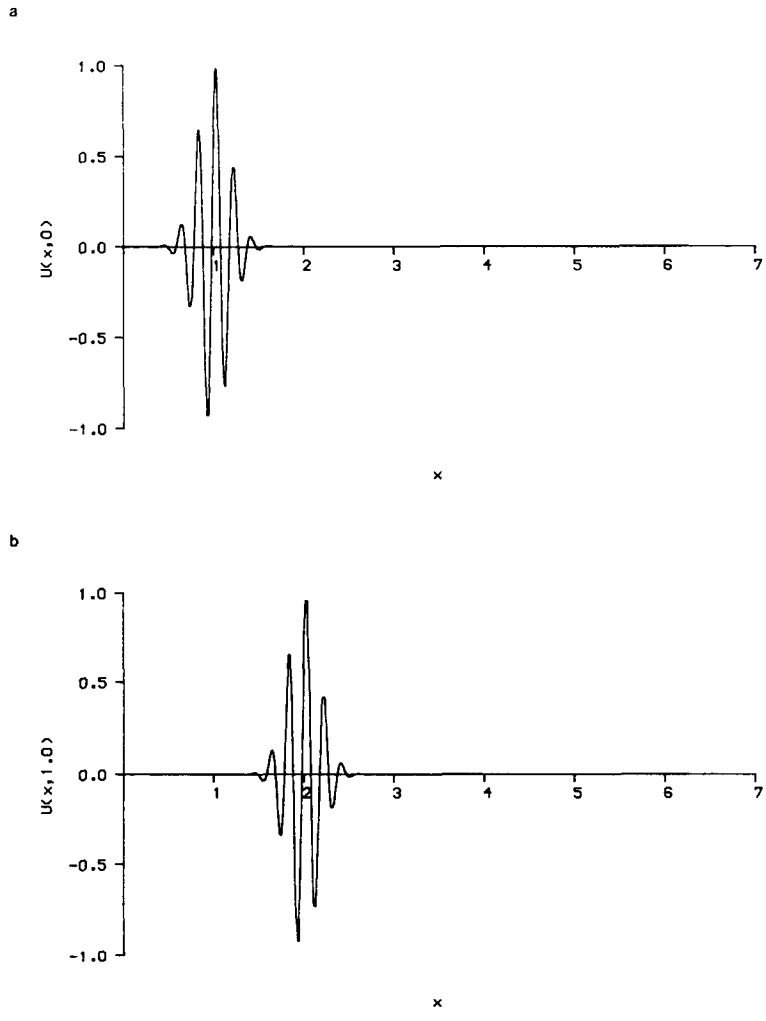

FIG. 3. Solutions of (2.16) with initial condition (2.34), $\mu = 1$, $m = 32$, $N = 256$, and filter (2.13): (a), (b), and (c) give the initial profile at $T = 0$, the unfiltered solution at $T = 1$, and the filtered solution at $T = 1$ with $K = 1/4096$, respectively.

This initial condition provides initial values $\hat{U}(p, 0)$ via (2.3) and the pseudospectral solution at time $t = T$ is then given by exact solution in Fourier space followed by Fourier inversion as in (2.4). We chose $m = 32$ and set N to 256 to give sufficient resolution of the high frequency wave. Results are displayed for the advection equation with $\mu = 1$, and filtering is performed by the exponential filter with $K = \frac{1}{4096}$. Equation (2.30) shows that the group velocities in unfiltered and filtered cases for this parameter set are, respectively, 1 and 0.39. Figure 3a shows the initial profile

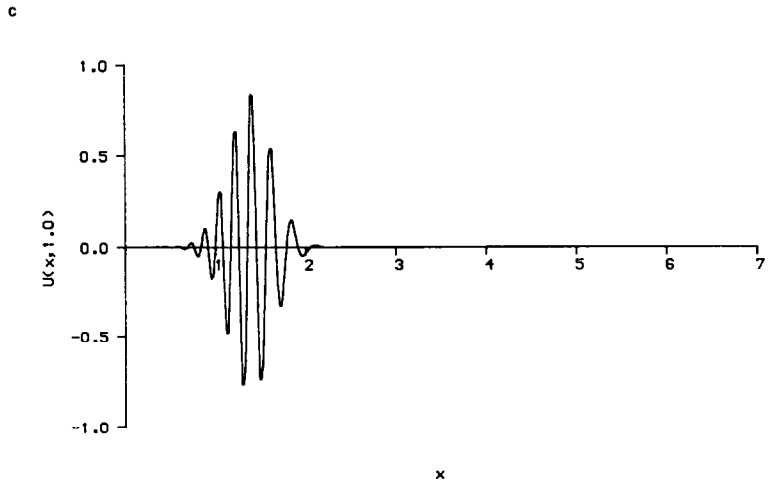

FIG. 3—*Continued*

(2.34) with the packet centred at $x=1$. Figure 3b shows the unfiltered solution at $T=1$ with the packet centred at $x=2$ and Fig. 3c shows the filtered solution at $T=1$ with the packet at $x=1.39$. Note also that the wave packet is wider in the filtered solution as a result of the induced dispersion.

3. Linear Equations and Chebyshev Methods

In this short section we present solutions of the linear Burgers equation

$$u_t + u_x = u_{xx}, \qquad (x, t) \in (-1, 1) \times (0, T] \tag{3.1a}$$

$$u(x, 0) = h(x), \qquad x \in [-1, 1] \tag{3.1b}$$

$$u(-1, t) = f(t), \qquad u(+1, t) = g(t), \qquad t \in (0, T] \tag{3.1c}$$

We seek a solution of the form

$$u_N(x, t) = \sum_{i=0}^{N} a_i(t)\, T_i(x), \tag{3.2}$$

where $T_i(x)$ is the Chebyshev polynomial of the first kind of degree i. Here the collocation equations are constructed by setting the residual of (3.1a) and (3.2) to zero at the Gauss–Lobatto points:

$$x_j = \cos(\pi j/N), \qquad j = 1, 2, \ldots, N-1. \tag{3.3}$$

Let $\mathbf{U}(t)$ be the $(N+1)$ component vector

$$[u_N(x_0, t), u_N(x_1, t), ..., u_N(x_N, t)]^T$$

and let $\mathbf{U}_x(t)$ and $\mathbf{U}_{xx}(t)$ be analogous vectors with components $(\partial U_N/\partial x)(x_j, t)$ and $(\partial^2 U_N/\partial x^2)(x_j, t)$ for $j=0, 1, ..., N$. It may be shown (see, for example, [2 or 9]) that

$$\mathbf{U}_x = (C^{-1}D^{(1)}C)\,\mathbf{U} \tag{3.4}$$

and

$$\mathbf{U}_{xx} = (C^{-1}D^{(2)}C)\,\mathbf{U}, \tag{3.5}$$

where $D^{(1)}$ and $D^{(2)}$ are the so-called differentiation matrices of first and second order, and C is the Chebyshev transformation matrix. C and C^{-1} are symmetric $(N+1)\times(N+1)$ matrices. If $[\mathbf{U}]_j$ denotes the jth component of the vector $\mathbf{U}$ we may write the collocation, or pseudospectral, equations as

$$\left[\frac{d\mathbf{U}}{dt}\right]_j = [(C^{-1}(D^{(2)} - D^{(1)})C)\mathbf{U}]_j, \qquad j=1, 2, ..., N-1. \tag{3.6}$$

This set is conjoined with the boundary conditions $[\mathbf{U}(t)]_0 = g(t)$ and $[\mathbf{U}(t)]_N = f(t)$ to give an inhomogeneous linear system of the form

$$\frac{d\mathbf{V}}{dt} = A\mathbf{V} + \mathbf{F}, \tag{3.7}$$

where $\mathbf{V}(t) = [U_N(x_1, t),\ U_N(x_2, t), ...,\ U_N(x_{N-1}, t)]^T$, $\mathbf{F}$ is a time-dependent $(N-1)$-vector, and A is an $(N-1)\times(N-1)$ constant matrix.

In a filtered Chebyshev pseudospectral approach we smooth the interpolant before differentiation. That is, prior ot the construction of spatial derivatives we multiply the coefficient a_i in (3.2) by a filter function β_i, where β_i is a decreasing function of i which satisfies

$$\begin{aligned} 0 \leqslant \beta_i \leqslant 1 \qquad & \text{for} \quad i=0, 1, ..., N; \\ \beta_i \simeq 1, \qquad & 0 \leqslant i \ll N; \\ \beta_i \ll 1, \qquad & i \simeq N. \end{aligned}$$

The effect of filtering is to replace the pseudospectral equations (3.6) by

$$\left[\frac{d\mathbf{U}}{dt}\right]_j = [(C^{-1}(D^{(2)} - D^{(1)})\,BC)\mathbf{U}]_j, \qquad j=1, 2, ..., N-1, \tag{3.8}$$

in which B is a diagonal $(N+1)\times(N+1)$ matrix with elements $\beta_0, \beta_1, ..., \beta_N$. This, of course, leads to a modification of (3.7). Unlike the Fourier case, the effect of filtering on the Chebyshev method cannot be put in terms of a simple modification to the partial differential equation. We propose to illustrate the effect of filtering by means of numerical computations.

The linear equation (3.7) was solved numerically for unfiltered and filtered derivatives using the fully implicit scheme

$$\frac{1}{\Delta t}[\mathbf{V}^{n+1}-\mathbf{V}^n]=\frac{1}{2}A[\mathbf{V}^{n+1}+\mathbf{V}^n]+\frac{1}{2}[\mathbf{F}^{n+1}+\mathbf{F}^n]$$

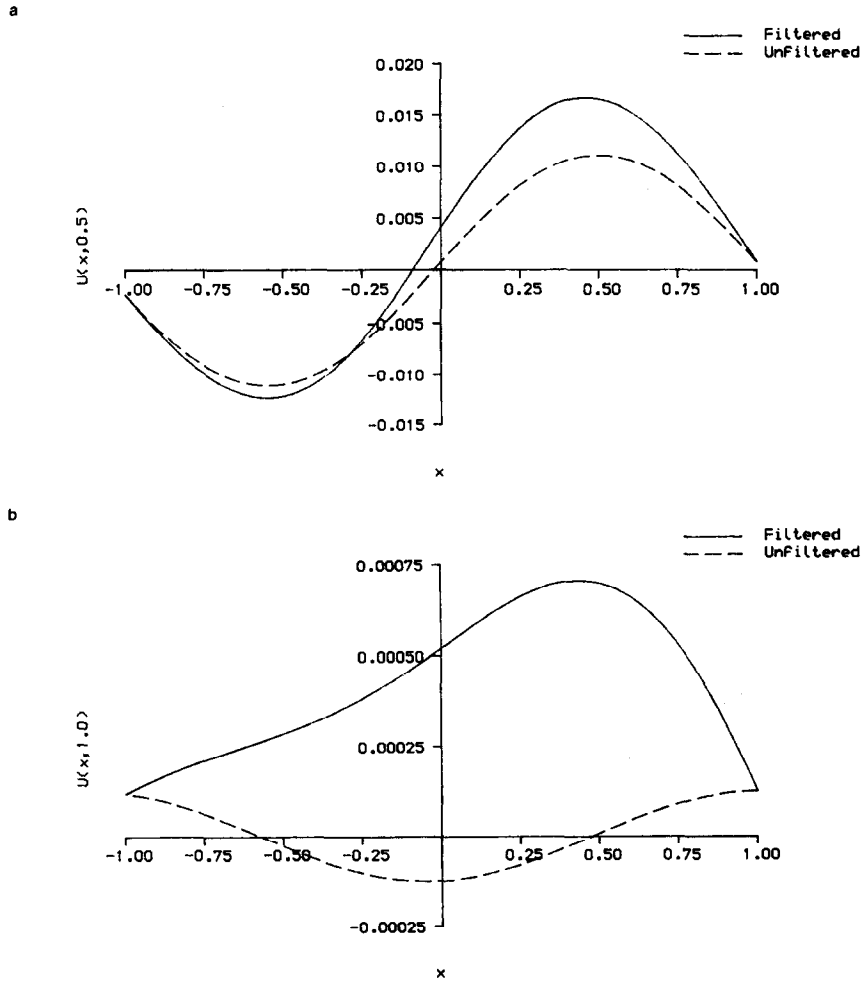

FIG. 4. Filtered and unfiltered solutions of (3.1), boundary conditions from (3.10) and filter $\beta_i=\exp(-i^2/100)$; (a) and (b) give solutions at $T=0.5$ and $T=1$, respectively.

or

$$\mathscr{A}\mathbf{V}^{n+1} = \mathbf{F}^n, \tag{3.9}$$

where $\mathbf{V}^n$ approximates $\mathbf{V}$ at $t = t_n = n\,\Delta t$. The time independent matrix $\mathscr{A}$ may be factorised before the start of the time evolution.

The scheme (3.9) was used to solve (3.1a), with initial and boundary conditions given by the exact solution

$$u(x, t) = e^{-9t}\cos[3(x-t)]. \tag{3.10}$$

In the filtered computations the exponential filter $\beta_i = \exp(-i^2/100)$ was used. Figures 4a, b show the computed solutions at times $T = 0.5$ and $T = 1.0$ obtained using $\Delta t = 0.001$ and $N = 64$. As in the case of Fourier filtering of the linearised Burgers equation, there is evidence of a diminution of the dissipation and of a phase shift. Of course, in this case there is also an effect arising from the boundary constraints which operates equally in unfiltered and filtered cases. Scheme (3.9) was also used to approximate a solution of (3.1a) with initial condition

$$u(x, 0) = x(x^2 - 1).$$

The results were qualitatively similar to those displayed in Figs. 4 in terms of reduction in dissipation and change in phase.

4. Nonlinear Solutions by Fourier Methods

4.1. *Induced Stability by Filtering*

Consider the nonlinear advection equation

$$v_t + (v + a)v_x = 0, \qquad (x, t) \in [-L, L] \times (0, T] \tag{4.1}$$

Here a is a real parameter and it is assumed that the solution u vanishes near the boundaries $x = \pm L$. For convenience we transform the spatial variable in (4.1) to $X = (\pi/L)(x + L)$ and seek a 2π-periodic solution $u(X, t)$ which satisfies

$$u_t + \rho(u + a)u_X = 0, \qquad (X, t) \in \mathbb{R} \times (0, T] \tag{4.2}$$

with ρ denoting π/L. As in Section 2.1 we approximate $u(\cdot, t)$ by $U(\cdot, t) \in \mathbb{R}^N$, which has the value $U(X_j, t)$ at $X = X_j = j\,\Delta X = 2\pi j/N$, $j = 0, 1, ..., N-1$. In the filtered case the pseudospectral scheme used here is a leap-frog scheme which may be written for $j = 0, 1, ..., N-1$ as

$$U(X_j, t + \Delta t) = U(X_j, t - \Delta t) - 2\rho\,\Delta t(U(X_j, t) + a)(F^{-1}(ip\sigma_p \hat{U}(p, t)))(X_j), \tag{4.3}$$

and this is replaced by an Euler step to compute $U(X_j, \Delta t)$, $j = 0, 1, ..., N-1$. For the unfiltered case we replace σ_p in (4.3) and in the Euler step by unity.

The focus of interest here is the interaction between the nonlinearity in (4.3) and the dispersion induced by the filtered derivative. If σ_p is the general filter function given by (2.7), then the argument leading to (2.8) shows that the filtered solution by (4.3) will be equivalent to an unfiltered pseudospectral solution of the modified equation

$$u_t + \rho(u+a)u_X + \rho(u+a)\sum_{s=1}^{\infty} a_s u^{(1+2s)} = 0, \tag{4.4}$$

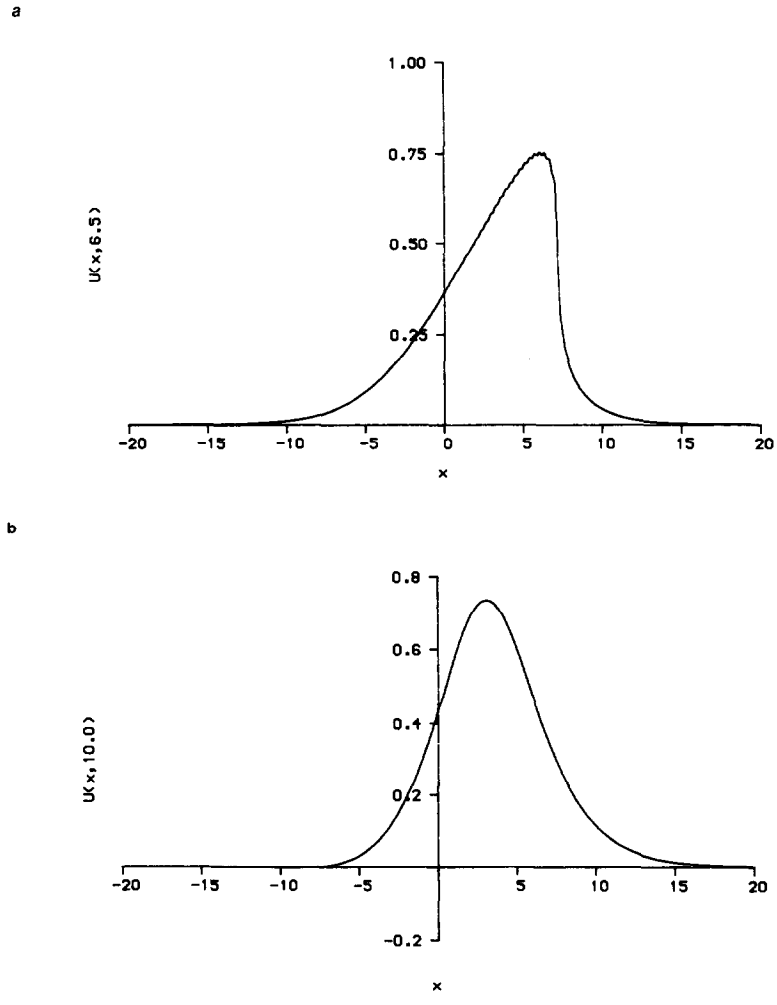

FIG. 5. Solutions of (4.1) with initial condition (4.6) and filter (2.13): (a) is unfiltered at $T = 6.5$; (b) is filtered at $T = 10$ and $K = 0.1$; (c) is filtered at $T = 5$ and $K = 0$, 0.01, 0.1; (d) is filtered at $T = 5$, $K = 0.1$, and $a = -1$, 0, 1.

where $u^{(r)}$ denotes the rth spatial derivative of u. All filtered computations described in this section were performed using the exponential filter $\sigma_p = e^{-Kp^2}$ and, in this case, the modified equation becomes

$$u_t + \rho(u+a)[u^{(1)} + Ku^{(3)} + \tfrac{1}{2}K^2u^{(5)} + \tfrac{1}{6}K^3u^{(7)} + \cdots] = 0. \tag{4.5}$$

For $K \ll 1$ this equation is in some respects similar to the KdV equation, and we are therefore interested in determining whether filtered solutions of (4.1) have any of the interesting properties associated with KdV solutions.

Equation (4.1) was solved with $a = 0.2$, $L = 20$ and the initial condition

$$v(x, 0) = 0.75 \operatorname{sech}^2(0.25x). \tag{4.6}$$

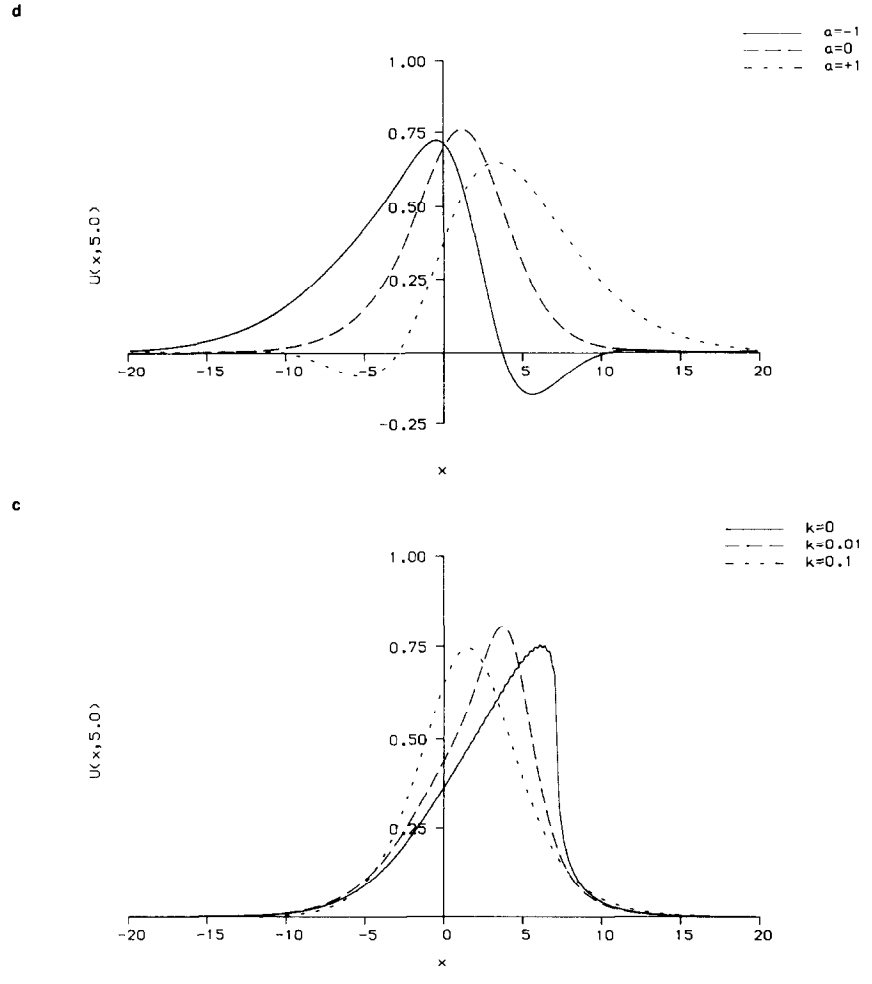

FIG. 5—*Continued*

Computations were performed using $\Delta t = 0.01$ and $N = 256$. The unfiltered solution at time $T = 6.5$, as displayed in Fig. 5a, shows clearly the steepening at the wave front, and shortly after this instant the wave becomes discontinuous. (The discontinuity develops slightly later, at approximately $T = 9$, in the exact solution of (4.1) and (4.6).) The solution filtered by $\sigma_p = e^{-p^2/10}$ is shown in Fig. 5b for the later time $T = 10.0$. This solution has a soliton-like appearance, with no steepening at the wave front. Figure 5c shows the solutions at time $T = 5.0$ obtained using the filter $\sigma_p = e^{-Kp^2}$, with $K = 0$, 0.01, 0.1. Note the tendency to soliton shape as K increases.

The filter introduces an additional feature to the solution, and this is a trough which develops and increases in depth as time evolves. At a given time the depth increases with $|a|$ and it occurs at the front or back of the wave according as $a < 0$ or $a > 0$. Figure 5d shows the trough at time $T = 5.0$ with $a = -1$, 0, 1 and filter constant $K = 0.1$. The trough does not occur if $a = 0$. Numerical experiments with $a = 1$ and several values of K indicate that the trough is a consequence of the filtering and it is not a property of the exact solution of the differential equation.

4.2. *Recurrence in Filtered Advection Solutions*

In Section 4.1 we observed that Fourier-filtered solutions of (4.1) displayed properties like those of the KdV equation. Here we pursue this analogy by investigating whether solutions of (4.1) might reproduce the recurrence phenomenon first described by Zabusky and Kruskal [12]. The reader is referred to the original paper for details.

To investigate the recurrence phenomenon we solved (4.1) for $0 \leqslant x \leqslant 2$, $t > 0$ using the initial condition $v(x, 0) = \cos(\pi x)$. The transformation to (4.2) is effected via $X = \pi x$, so that $\rho = \pi$ in the difference scheme (4.3). All computations were performed using the exponential filter with constant $K = 0.01$, and with discretisation parameters $\Delta t = 0.001$ and $N = 256$.

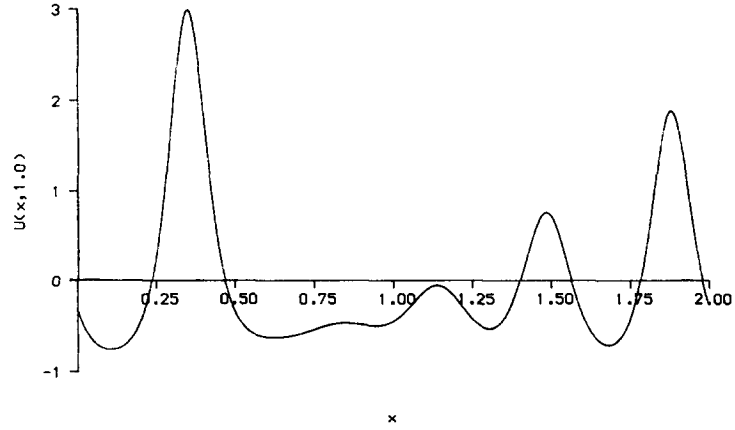

FIG. 6. Solution of (4.1) at time $T = 1$, with initial condition $\cos(\pi x)$, $a = 2$, and filter (2.13) with $K = 0.01$.

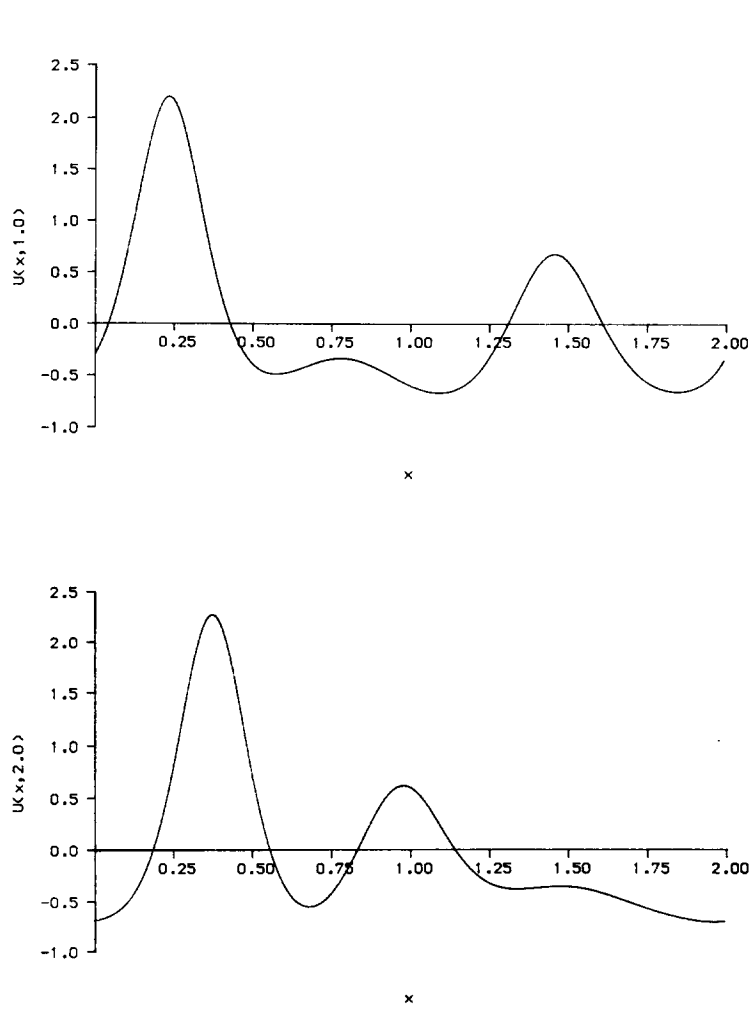

FIG. 7. Solution of (4.1) at various times with initial condition $\cos(\pi x)$, $a = 6$, and filter (2.13) with $K = 0.01$: (a) $T = 1$; (b) $T = 2$; (c) $T = 2.7$, first recurrence; (d) $T = 4$; (e) $T = 5$; (f) $T = 5.38$, second recurrence.

Figure 6 shows the solution of (4.1) with $a = 2$ at time $T = 1.0$. By this time the profile shows several solitons. We conducted extensive numerical experiments which revealed, inter alia, that solitons pass through each other without noticeable distortion and that the propagation velocity of a soliton is proportional to its amplitude.

Figures 7a–f show the solution corresponding to $a = 6$ at several values of time. Figures 7a, b show three solitons at times $T = 1.0$ and $T = 2.0$; in Fig. 7c the solitons have coalesced at $T = 2.70$ to produce a profile which resembles the original cosine,

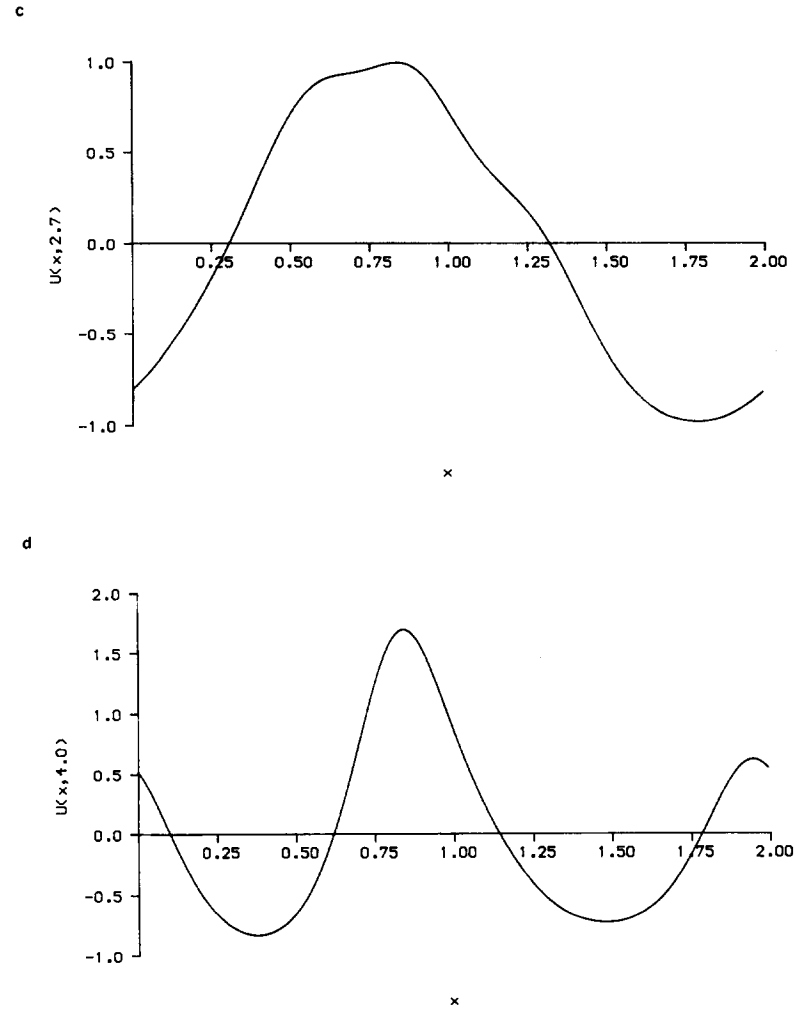

albeit with a phase shift. This recurrence is repeated in Figs. 7d, e, f, where the profiles are shown at times $T = 4.0$, 5.0, and 5.38. The results displayed in Figs. 7c, f suggest that a phase-shifted cosine profile is produced at integer multiples of a recurrence time T_R, where T_R is approximately 2.7 for $a = 6$.

To emphasize the stabilising effect of the filtering process we have shown the unfiltered solution for $a = 6$ at time $T = 0.35$. At this time the unfiltered solution is about to become discontinuous at the wave front. The global accuracy of Fourier spectral solutions of linear hyperbolic systems with discontinuous initial data has been examined in detail by Majda, McDonough, and Osher [8]. They have shown that the Fourier method is globally inaccurate in the absence of proper smoothing.

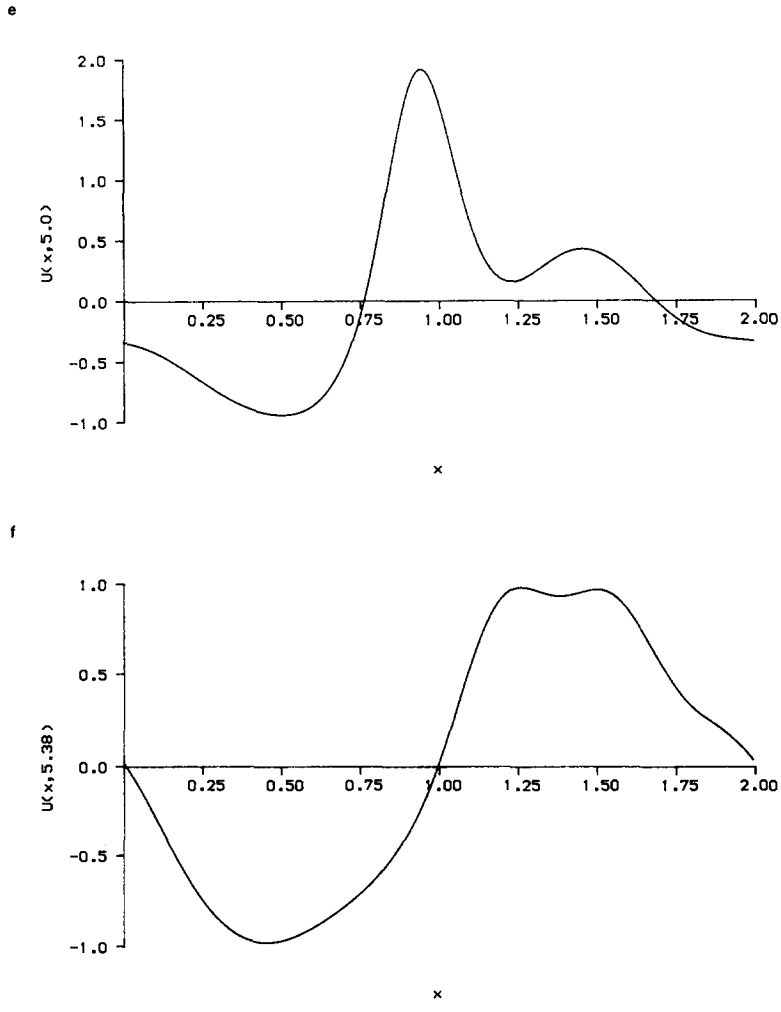

FIG. 7—*Continued*

In regions which exclude the discontinuity the accuracy is reduced to $O(N^{-2})$ for any $t>0$. Majda *et al.* have shown, however, that spectral accuracy can be recovered away from the discontinuity if appropriate filtering is applied. In the constant coefficient case they have shown that suitable filtering of the continuous Fourier coefficients of the initial data will suffice, since there is no mechanism for the generation of high frequency modes during the time evolution. In the case of variable coefficients, however, this initial-data smoothing has to be supplemented by a filtering of the discrete Fourier coefficients in the formation of spatial derivatives as time evolves.

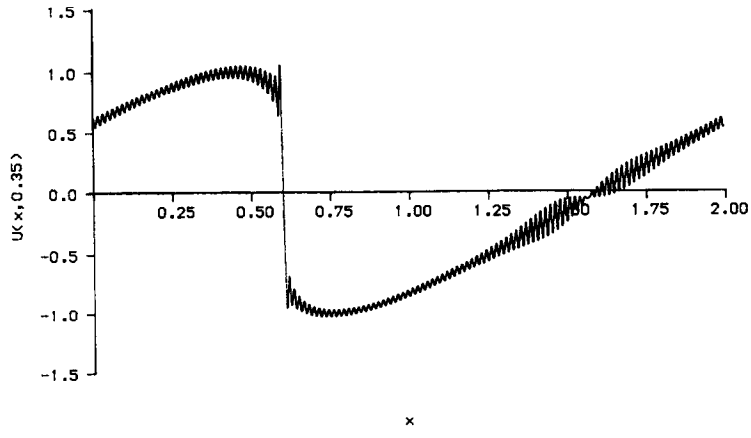

FIG. 8. Unfiltered solution of (4.1) at time $T=0.35$ with initial condition $\cos(\pi x)$ and $a=6$.

5. CONCLUSIONS

Filtered Fourier pseudospectral solutions of linear, time-dependent partial differential equations are considered. It is shown that if the spatial derivatives are filtered the effect is to produce a solution of a modified differential equation. This modification may introduce false dispersion, or diffusion, depending on the structure of the original spatial differential operator. Numerical results are presented to illustrate these effects. Results are also presented on filtered Chebyshev pseudospectral solutions. There, too, the effects of false dispersion and dissipation are evident.

The effect of filtering on pseudospectral solutions of the nonlinear advection equation is examined. Numerical results show that the interaction between nonlinearity and false dispersion is capable of producing solutions which have some soliton properties. This fascinating interaction is also capable of producing numerical solutions of the advection equation which exhibit the Zabusky–Kruskal [12] recurrence phenomenon. However interesting the spurious soliton solutions might be one should not lose sight of the main objective associated with filtering. It should be stressed that filtering is introduced to control the growth of high frequency modes and that this is done at the cost of accuracy loss in the low modes. A proper choice of filter is a compromise between these competing effects. It is hoped that the results presented here will give further insight into the effects of filtering on pseudospectral solution of evolutionary partial differential equations and that this might contribute to the construction of acceptable filters.

ACKNOWLEDGMENTS

One of us (LSM) wishes to acknowledge the receipt of a Science and Engineering Research Council Studentship.

REFERENCES

1. B.-Y. GUO AND W.-M. CAO, *J. Comput. Phys.* **74**, 110 (1988).
2. C. CANUTO, M. Y. HUSSAINI, A. QUARTERONI, AND T. A. ZANG, *Spectral Methods in Fluid Dynamics* (Springer-Verlag, New York/Berlin, 1987).
3. M. DUBINER, *J. Sci. Comput.* **2**, 3 (1987).
4. B. FORNBERG AND G. B. WHITHAM, *Phil. Trans. R. Soc. London* **289**, 373 (1978).
5. S. R. FULTON AND G. D. TAYLOR, *J. Comput. Phys.* **55**, 302 (1984).
6. D. GOTTLIEB AND E. TURKEL, *Stud. Appl. Math.* **63**, 67 (1980).
7. H.-P. MA AND B.-Y. GUO, *J. Comput. Phys.* **65**, 120 (186).
8. A. MAJDA, J. MCDONOUGH, AND S. OSHER, *Math. Comput.* **32**, 1041 (1978).
9. F. Z. NOURI, Ph.D. thesis, University of Strathclyde, Glasgow, UK, 1988 (unpublished).
10. S. A. ORSZAG, *Stud. Appl. Math.* **50**, 293 (1971).
11. J. A. C. WEIDEMAN AND L. N. TREFETHEN, *SIAM J. Numer. Anal.* **25**, 1279 (1988).
12. N. J. ZABUSKY AND M. D. KRUSKAL, *Phys. Rev. Lett.* **15**, 240 (1965).